

October 24, 2018
arXiv:xxxx.yyyy [hep-ph]
LAPTH-1259/08
IMSc-2008/06/11
LPT-Orsay-08-59

Jet-jet and hadron-jet correlations in hadro- and electro-production

P. Aurenche¹, Rahul Basu², M. Fontannaz³

¹*LAPTH*, Université de Savoie, CNRS,
B.P.110, F-74941 Annecy-le-Vieux Cedex, France*

²*The Institute of Mathematical Sciences,
Chennai 600 113, India*

³*Laboratoire de Physique Théorique, UMR 8627 CNRS,
Université Paris XI, Bâtiment 210, 91405, Orsay, Cedex, France*

Abstract

We discuss, in the framework of perturbative QCD at next to leading order, two related observables which are usually considered to provide tests of the BFKL dynamics : jet-jet correlations at Tevatron energies and forward particle-jet correlations at HERA. In the first case we study the rapidity gap dependence of the azimuthal correlations and find slightly too strong correlations at large gap. In the second case we discuss the cross section as well as the azimuthal correlations over a rapidity gap range of 5 units. We find that the requirement of a forward particle imposes strong kinematical constraints which distort the distributions, notably at small rapidity gaps. We also show that the decorrelation is stronger in electroproduction than in hadron-hadron collisions. Unfortunately no data are yet available for comparison.

*Laboratoire d'Annecy-le-Vieux de Physique Théorique, UMR 5108 du CNRS.

1 Introduction

The first test of BFKL [1] dynamics in hadronic collisions was proposed by Mueller and Navelet [2] who showed that the cross section for the inclusive production of 2 jets at the partonic level would increase exponentially with the rapidity separation, $\Delta\eta$, of the jets. At the hadronic level the cross section involves a convolution with the initial parton distributions, as a result of which the hadronic cross section decreases with the rapidity gap due to the very fast fall-off of the parton densities. In order to disentangle the interesting dynamical effects from the parton distributions effect the study of the normalized azimuthal angle distribution [3, 4] was proposed which should be less sensitive to the latter. More precisely, the relevant quantity to consider is the average $\langle \cos(\pi - \phi) \rangle$, where ϕ is the azimuthal angle between the 2 jets. From BFKL dynamics one would expect a very fast decorrelation, due to the emission of a growing number of jets in the rapidity interval between the observed jets. This is to be contrasted to the case of DGLAP [5] dynamics as implemented in lowest order (LO) and next-to-lowest order (NLO) calculations: at LO the 2 jets are perfectly correlated ($\phi = \pi$) while at NLO the decorrelation arises from the emission of just one extra jet. Monte-Carlo codes based on DGLAP dynamics offer however the possibility of a stronger decorrelation due to parton showers.

Coming back to BFKL dynamics it was noted [6, 7, 8] that the predictions were very sensitive to energy momentum constraints neglected in the original analytic calculations. This is, in particular, true for azimuthal correlations where an exact energy momentum conservation considerably softens the rapidity dependence, compared to the analytical (asymptotic) results. Indeed, less phase space is available for the emission of intermediate gluons in the former case. Because of these and other effects [8, 9] the BFKL predictions show less decorrelation than that found in the initial calculations.

Data on $\langle \cos(\pi - \phi) \rangle$ at Tevatron energies have been obtained by the DØ collaboration [10] in the range $0 < \Delta\eta < 5$ and have been compared to a variety of calculations. The leading order BFKL asymptotic predictions are completely ruled out by the data while the leading order ones, including energy momentum conservation [6, 8], or the next-to-leading order ones [9] are closer

to the data with still a too strong rapidity decrease. On the other hand, the NLO predictions of JETRAD [11] do not show enough decorrelation as the rapidity increases. Only the HERWIG [12] results are in very good agreement with the data.

BFKL dynamics can also be probed by considering the cross section for forward production of a large p_{\perp} jet or particle in deep-inelastic scattering (DIS) events at small Bjorken- x x_{Bj} [13], in the domain $p_{\perp}^2 \sim Q^2$. Such data have been collected by the H1 [14, 15] and ZEUS [16] collaborations. For this observable, models based on BFKL dynamics (supplemented by some phenomenological inputs) [17], were claimed to be in reasonable agreement with data although they did not account for the correct Q^2 evolution. More recently, several NLO calculations of forward π^0 production have been carried out [18, 19, 20, 21, 22, 23] and found in agreement with the latest H1 data [15]: in particular, the dependence of the cross section as a function of the variables x_{Bj} , Q^2 , x_{π} , p_{\perp}^* (where x_{π} and p_{\perp}^* are, respectively, the fraction of longitudinal momentum and the transverse momentum of the pion in the γ^* -proton center of mass frame) are very well reproduced [20].

To further study the validity of the perturbative approach in deep-inelastic scattering, we propose to consider azimuthal correlations involving a forward large p_{\perp} hadron, to probe the small x_{Bj} where BFKL dynamics is often thought to be more relevant. Because of the different subprocess structure, it is interesting to compare the azimuthal correlations in hadroproduction and in electroproduction. However, in the latter case, the perturbative dynamics is more complex because the cross section is built from two contributions, the so-called direct and resolved contributions.

In the following section, we first go back to correlations in $p\bar{p}$ collisions at the Tevatron, from a perturbative point of view, and find that the rapidity dependence, quite sensitive to scale changes, is within the experimental errors, although being not steep enough. In Sect. 3 we turn to DIS and study forward-pion jet correlations. We consider two classes of observables: the cross section and the average $\langle \cos(\pi - \phi) \rangle$ as a function of the rapidity hadron-jet separation for different Q^2 values. The importance of kinematical constraints on the shape of the rapidity distribution is stressed. Conclusions are given in a final section.

2 Azimuthal correlations in hadron-hadron collisions

The DØ collaboration measured [10] the rapidity dependence of the azimuthal correlations between large- p_{\perp} jets at $\sqrt{s} = 1800$ GeV with the following criteria: among the jets with $E_{\perp} > 20$ GeV, the two jets having the largest and the smallest pseudorapidity were selected. One of the two jets was also required to be above 50 GeV. The selected jets are required to be in the pseudorapidity range $|\eta_{1,2}| \leq 3$ and the azimuthal correlations are measured as a function of $\Delta\eta = \eta_1 - \eta_2$. More precisely, DØ measures $\langle \cos(\pi - \phi) \rangle$ as a function of $\Delta\eta$ where ϕ is the azimuthal angle between the two jets.

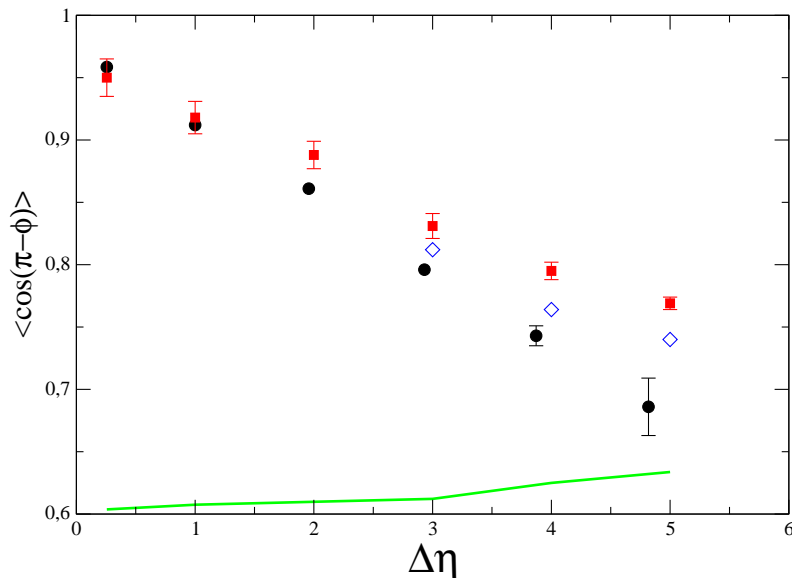


Figure 1: Theoretical predictions, at NLO in perturbative QCD, of the two-jet correlations (squares: scale $P_{\perp}/2$; diamonds: scale $P_{\perp}/4$) compared with DØ data [10] (solid dots). The solid line indicates the systematic errors.

To study this quantity we use the code DIJET which belongs to the PHOX Family [24] and calculate single jet and dijet cross sections at NLO in hadron-hadron collisions. The interested reader may find technical details on the PHOX Family codes on the site [24]. We have checked that the DIJET predictions are in good agreement with the single jet cross section of ref. [25] and with the spectrum $dN/d\Delta\eta$ measured by DØ [10] under the conditions described above. The

parton distribution functions are CTEQ6M [26] and we use $P_{\perp}/2$ as the standard factorization and renormalization scales, where P_{\perp} is half the sum of the transverse momenta of the largest p_{\perp} partons, $P_{\perp} = \frac{p_{\perp 1} + p_{\perp 2}}{2}$. For the jets we use $R_c = .7$ and $R_{sep} = 1.3 R_c$ as in ref. [25].

We now focus on the azimuthal correlations. We calculate the values of $\langle \cos(\pi - \phi) \rangle$ quoted by the DØ collaboration in Fig. 4 of ref. [10]. We expect the corresponding theoretical predictions to be sensitive to the choice of scales. Indeed the aplanarity of the jets is due to the $2 \rightarrow 3$ subprocesses and when ϕ is different from π we perform a LO calculation. Only the region $\phi \sim \pi$ corresponds to a full NLO calculation. To test this sensitivity we start with the standard scale $P_{\perp}/2$. The result is displayed in Fig. 1 (squares) together with the DØ data (solid dots). The theoretical error due to the limited statistics in the Monte Carlo integration is of the order of $\pm 10\%$ or less.

Another scale which may appear more natural is (minus) the square of the momentum transfer in the t -channel of a $2 \rightarrow 2$ subprocess, $Q^2 = p_{\perp}^2 (1 + e^{-(\eta_1 - \eta_2)})$, p_{\perp} being a jet transverse momentum. In order to have a scale close to $p_{\perp}/2$ when $\eta_1 \sim \eta_2$ we use $c P_{\perp} \left(\frac{1 + e^{-(\eta_1 - \eta_2)}}{2} \right)^{\frac{1}{2}}$ with $c = \frac{1}{2}$ for the factorization and the renormalisation scales. We obtain results almost identical to those obtained with the scale $P_{\perp}/2$ (about 1% lower). Finally with the scale $P_{\perp}/4$ we get the results shown by the diamonds in Fig. 1.

The agreement between data and theory is not perfect, the theoretical points staying at the upper limit of the experimental error (statistical + systematic). The smooth decrease of $\langle \cos(\pi - \phi) \rangle$ with increasing $\Delta\eta$ is well reproduced at small and medium rapidity gaps, but at large $\Delta\eta$ the jets in the NLO calculation appear to be too much correlated. Note that with the scale $\sum_{i=1}^3 p_{\perp i}/2$ we recover the JETRAD results quoted in [10].

Other approaches based on the generator Herwig [12] and on a BFKL calculation [6] are also displayed by the DØ collaboration. The Herwig results are in good agreement with data whereas the BFKL prediction undershoots them by a large amount. A recent BFKL analytic calculation at next to leading order [9] gives a somewhat better description than the leading order one of Del Duca and Schmidt quoted in [10] which takes into account some non asymptotic effects.

The conclusion of this study is that HERWIG, and to a lesser extent NLO calculations, can give

a satisfactory description of the data, although the underlying dynamics is different. In the NLO calculation the jet aplanarity comes from the $2 \rightarrow 3$ subprocesses described by exact QCD matrix elements. These matrix elements are not present in HERWIG where the aplanarity comes from the initial and final parton showers. This mechanism leads to a correct value of $\langle \cos(\pi - \phi) \rangle$. (However the cross section for three large- p_{\perp} jets is expected to fall an order of magnitude below data, because of the lack of exact $2 \rightarrow 3$ matrix elements in this approach). Based on this analysis, we speculate that a NNLO calculation would give a satisfactory description of the data.

3 Hadron-jet azimuthal correlations in DIS

In ref. [20] we carried out a detailed study of single inclusive forward π^0 production in deep inelastic scattering and compared the NLO perturbative results with the recent H1 data (see ref. [14, 15] for experimental details and cuts). The data probe a small x_{Bj} range, $1.1 \cdot 10^{-4} < x_{Bj} < 1.1 \cdot 10^{-3}$ where DGLAP dynamics may break down. The calculation includes the "direct" component (where the virtual photon couples to the hard processes) and the "resolved" one where the photon acts as a composite object, both contributions being calculated at the next to leading order. We use the FORTRAN code DISPHOX developed from the real photoproduction code JETPHOX [24] and described in refs. [18, 19, 20] with the following inputs: the proton structure functions are taken from the CTEQ6M tables [26], the parton fragmentation functions into pions are those of KKP [27] while, for the resolved case, the photon structure functions are found in [19]. We work in the \overline{MS} renormalization and factorization schemes and all the scales are equal to $(Q^2 + p_{\perp}^2)$. We take $n_f = 4$ flavors and $\Lambda_{\overline{MS}} = 326$ MeV.

In Fig. 2 we display the single inclusive forward pion distribution as a function of x_{Bj} and its comparison with the various theoretical components of the cross section. A remarkable fact is the smallness of the Born direct term and the very large size of the higher order correction to this Born term (see [20] for a precise definition of various components). As already noted, at lowest order, the hard processes are mediated by quark exchange while, at higher orders, there appear diagrams with a gluon exchange in the t channel, *e. g.* $\gamma q \rightarrow qq\bar{q}$: because of the gluon pole these terms are enhanced in the case of forward production of hadrons and they considerably increase

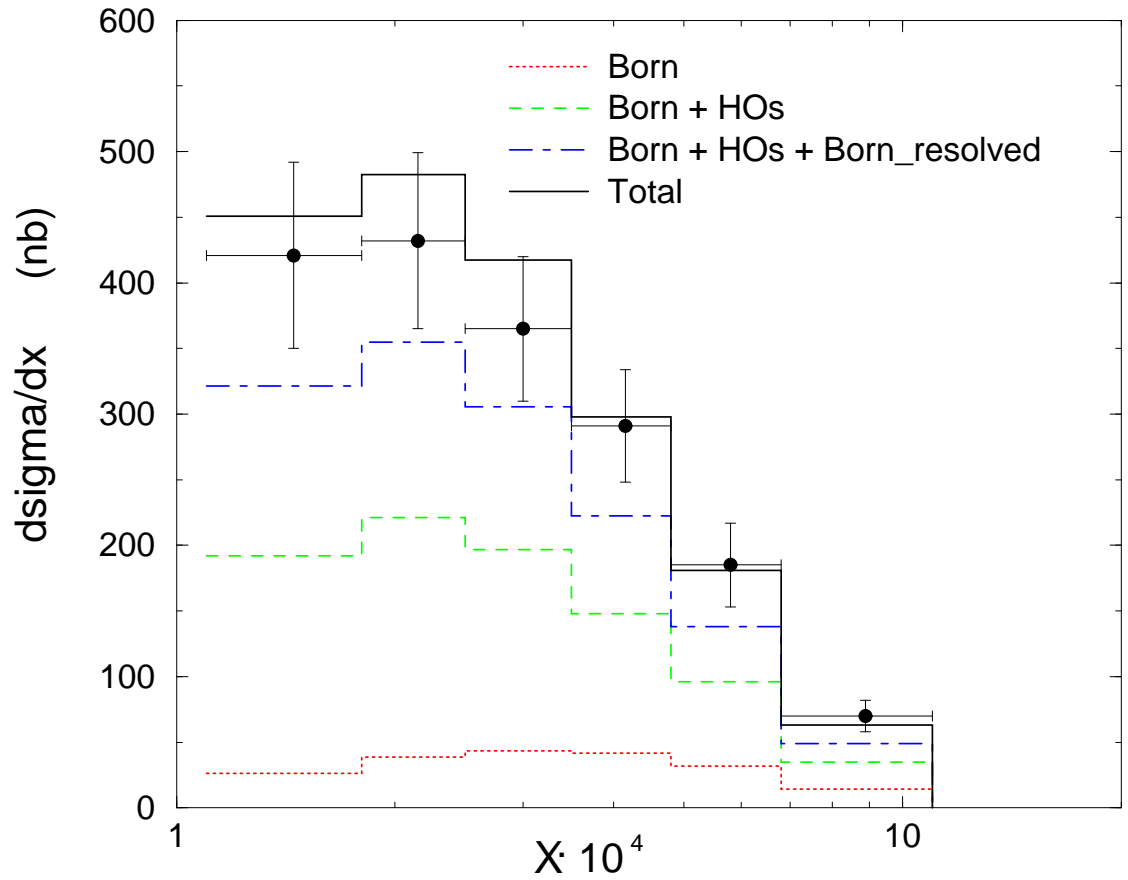


Figure 2: The cross section $d\sigma/dx_{Bj}$ corresponding to the range $4.5 \text{ GeV}^2 \leq Q^2 \leq 15 \text{ GeV}^2$ compared to H1 data [14]. The various theoretical components of the cross section are shown. The symbol HO_s denotes the HO correction from which the lowest order resolved contribution has been subtracted.

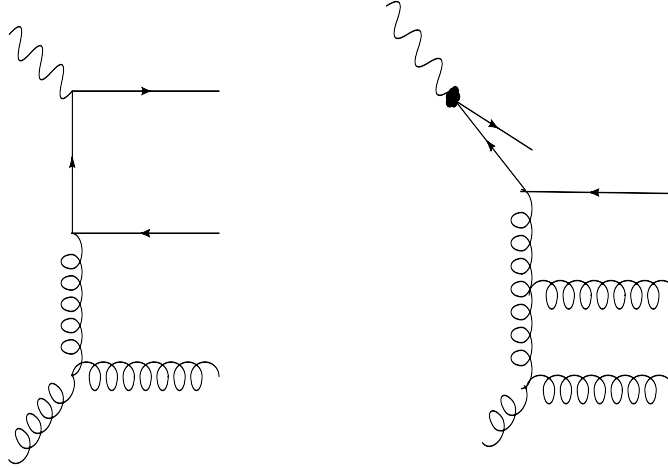


Figure 3: Examples of higher order corrections to (a) the direct contribution, (b) the resolved contribution. The forward hadron is emitted from the bottom parton line.

the production rate. The importance of the resolved component can also be explained along the same lines because, already at lowest order, it contains processes with a gluon exchange. In that case, the hard processes, at LO and NLO, are the same as in $p\bar{p}$ collisions, the only difference with the latter case being the convolution with the structure functions: those of the photon are less steep than those of the proton and the relative weight of gluon and quark initiated processes are different. In Fig. 3, we show two diagrams characteristic of the higher order corrections included in our calculation: it is clear that these diagrams can be seen as the lowest order terms of the BFKL ladder stretched between the photon (backward direction) and the proton (forward direction). If the available phase space (rapidity) between the forward and backward partons is large enough then multiple gluon emission is expected and the BFKL dynamics should dominate. In the opposite case the emission of one (or two) gluons is probably more appropriate. The very good agreement between the inclusive H1 data [15] and our perturbative calculation [20] seems to support the latter hypothesis which can be further tested by considering forward hadron-jet azimuthal correlations.

The H1 collaboration has studied azimuthal correlations between the highest two transverse momentum jets [28] in DIS events at small x_{Bj} . They find a reasonable agreement with perturbative calculations except for small separations in azimuth where models based on BFKL dynamics fare

better. Unlike the analysis in $p \bar{p}$ collisions they do not study the correlations between largest rapidity gap jets nor do they measure $\langle \cos(\pi - \phi) \rangle$ as a function of the rapidity gap.

In the following we study particle-jet correlations and we use the same DISPHOX code which was successfully used to describe the single inclusive forward pion data and we concentrate on the rapidity dependence of cross sections and $\langle \cos(\pi - \phi) \rangle$. Electron-jet correlations have already been considered in [29, 30] in the framework of the BFKL approach. In contrast to [29, 30], we propose to measure the forward hadron-jet correlations in which the trivial effect of the electromagnetic vertex is not present. These correlations are also closer to those measured in hadron-hadron collisions.

The momentum of a large- p_{\perp} final state is better fixed in experiments measuring hadrons than in those measuring jets. In the latter case, the link between jet and parton momenta are obtained via Monte-Carlo calculations and it might not be well controlled for small transverse momentum jets, with $p_{\perp} < 4$ GeV/c say. Besides, using a particle rather than a jet also allows us to extend the useful rapidity range of the observable.

All our results will be presented in the hadronic center of mass frame (CM*) where the virtual photon and initial parton in the proton are aligned along the z axis. The reason is the following. In the laboratory frame the photon has a transverse momentum $(\vec{q}_{\perp}^2 = (1-y)Q^2)^{\dagger}$ and therefore it can emit a collinear parton which can be part of a large- p_{\perp} jet. In the resolved case this parton is also collinear to the spectator partons contained in the photon and these latter must also be part of a large- p_{\perp} jet. As a result, large- p_{\perp} jets defined in the laboratory frame can be made of spectator partons, and we would need to modify the jet algorithm used in DISPHOX which only considers jets made of active partons (produced in the subprocess). Besides, the cross section would be very sensitive to the position of the cone (defining the jet) with respect to the photon momentum. For instance, a cone tangent to the photon momentum will lead to a “collinear divergent” (the quotation marks indicate that the divergence is actually regularized by the photon virtuality) cross section and factorization is broken. In order to avoid such pathologies, we never work in the laboratory frame and we impose, to insure the applicability of perturbation theory, a minimum

[†] y is the inelasticity of the electron $y = q \cdot P / P_e \cdot P$, with P_e and P the initial electron and proton momenta respectively.

value on the transverse momentum of particles measured in the CM* frame.

For our calculation we use the following cuts, in agreement with the H1 detector constraints. The lepton inelasticity is limited by $0.1 \leq y \leq 0.7$ and the Bjorken variable by $1. \leq 10^4 x_{Bj} \leq 5$. The forward π^0 is observed in the laboratory in the domain $5^\circ \leq \theta_\pi^{\text{lab}} \leq 25^\circ$ with a scaled energy $.01 \leq x_\pi = E_\pi^{\text{lab}}/E_p^{\text{lab}} \leq 1$. Furthermore we impose, in the CM* frame, $p_\perp^{*\pi} \geq 4$ GeV and $p_\perp^{*\text{jet}} \geq 3.5$ GeV. This last cut is defined to avoid too large higher-order corrections in some regions of phase space. The range of Q^2 is limited to 50 GeV^2 and, in our study, we vary the lower bound from 2 GeV^2 upward.

Before presenting the results it is worthwhile to discuss the constraints imposed by the above cuts. First, let us recall the necessary conditions for the BFKL dynamics to be relevant: one should maximize the rapidity extent of the photon-parton system. If \widehat{W} be the energy of this system, we should maximize the quantity (we recall the relation $yS = Q^2/x_{Bj}$):

$$\frac{\widehat{W}^2}{\sqrt{Q^2 p_\perp^*}} = \frac{\sqrt{Q^2}}{p_\perp^*} \frac{(x_1 - x_{Bj})}{x_{Bj}} = \frac{\sqrt{yS}}{p_\perp^*} \frac{(x_1 - x_{Bj})}{\sqrt{x_{Bj}}} \quad (3.1)$$

where S is the total electron-proton energy squared, x_1 the fraction of the proton momentum carried by the struck parton and p_\perp^* the transverse momentum of the final state parton. As is well known, this is achieved by using large y and small x_{Bj} , for p_\perp^* not too large. Considering the Born term kinematics with two hard partons in the final state, we can derive the following relation in the CM* frame

$$\exp(2\eta_\pi^* - \Delta\eta^*) = x_1 - \frac{Q^2(1 - x_1)}{yS - Q^2} = \frac{x_1 - x_{Bj}}{1 - x_{Bj}} \sim x_1 - x_{Bj} , \quad (3.2)$$

where η_π^* is the rapidity of the observed forward pion in the CM* frame and $\Delta\eta^*$ the rapidity gap between the pion and the jet. The angular conditions on the forward pion constrain the pion rapidity in the laboratory, $1.50 \leq \eta_\pi^{\text{lab}} \leq 3.13$, or approximately[‡] in the CM* frame $-.65 \leq \eta_\pi^* \leq 1$. When looking at the pion-jet correlations, if we further impose the condition of a forward going jet, $\Delta\eta^*$ decreases and x_1 increases. Therefore the condition $\Delta\eta^*$ small corresponds to a forward jet implying a large value of x_1 where the proton structure function is suppressed. Another relation

[‡]In the CM* frame, the pion rapidity is approximately ($Q^2 \ll p_\perp^{*2}$) given by $\eta_\pi^* = \eta_\pi^{\text{lab}} - 1.7 + \frac{1}{2} \ln y$ and we have used $\frac{1}{2} \ln y \sim -.46$ for $y \sim .4$

is (for $x_{Bj} \ll x_1$)

$$p_{\perp}^2 \cosh^2 \frac{\Delta\eta^*}{2} = \frac{Q^2}{4} \frac{(x_1 - x_{Bj})}{x_{Bj}} = \frac{x_1 y S - Q^2}{4} \sim x_1 y \frac{S}{4} . \quad (3.3)$$

showing that at large values of $\Delta\eta^*$ correspond large values of y (and small values of x_1 by eq. 3.2) which are cut by the condition $y < .7$.

These features can be clearly seen in Figs. 4 where the jets are defined as those with the largest transverse momentum. No rapidity plateau appears in the $\Delta\eta^*$ dependence of the cross section and the maximum of the cross section moves to larger values of $\Delta\eta^*$ when Q_{min}^2 , and correspondingly y , increases, as expected. In these figures it is worth noting that the resolved cross section, the relative weight of which decreases with increasing Q^2 , is less affected by the kinematics constraints discussed above in the Born case. Because it involves an extra convolution with the parton distribution functions in the photon, it is flatter than the direct contribution.

Some of the kinematical issues can also be understood by writing y and x_1 in terms of the rapidity of the final partons y_1 and y_2 . In a frame in which the proton and photon are collinear (P is the proton momentum in this frame)

$$y = \frac{p_{\perp}^*}{\sqrt{S}} \frac{2P}{\sqrt{S}} (e^{-y_1} + e^{-y_2}) \quad (3.4)$$

and

$$x_1 = \frac{p_{\perp}^*}{\sqrt{S}} \frac{\sqrt{S}}{2P} (e^{y_1} + e^{y_2}) + x_{Bj} \quad (3.5)$$

These equations directly give the variations of x_1 and y in terms of the rapidity of the final state jets and thereby the dependence of the parton distributions of the proton and the photon on these rapidities. Thus, a second forward parton corresponds to a larger value of x_1 whereas a backward parton corresponds to a larger value of y . These kinematical domains are thus suppressed by the large x_1 and large y behaviour of the proton and photon distribution functions respectively. Moreover, in the resolved case, eq.(3.4) is modified by multiplying the y on the LHS by an extra convolution z due to the further splitting of the photon into a $q\bar{q}$ pair. Thus, for the direct case, y_2 is determined by Q^2 , y and y_1 which also determines the cross section. In the resolved case,

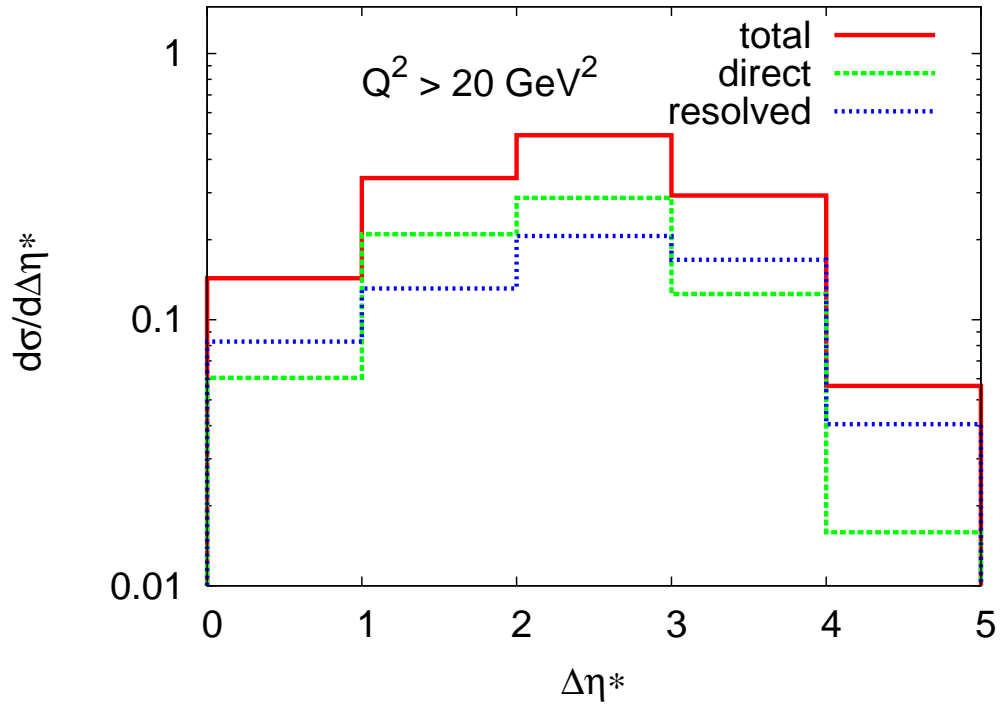
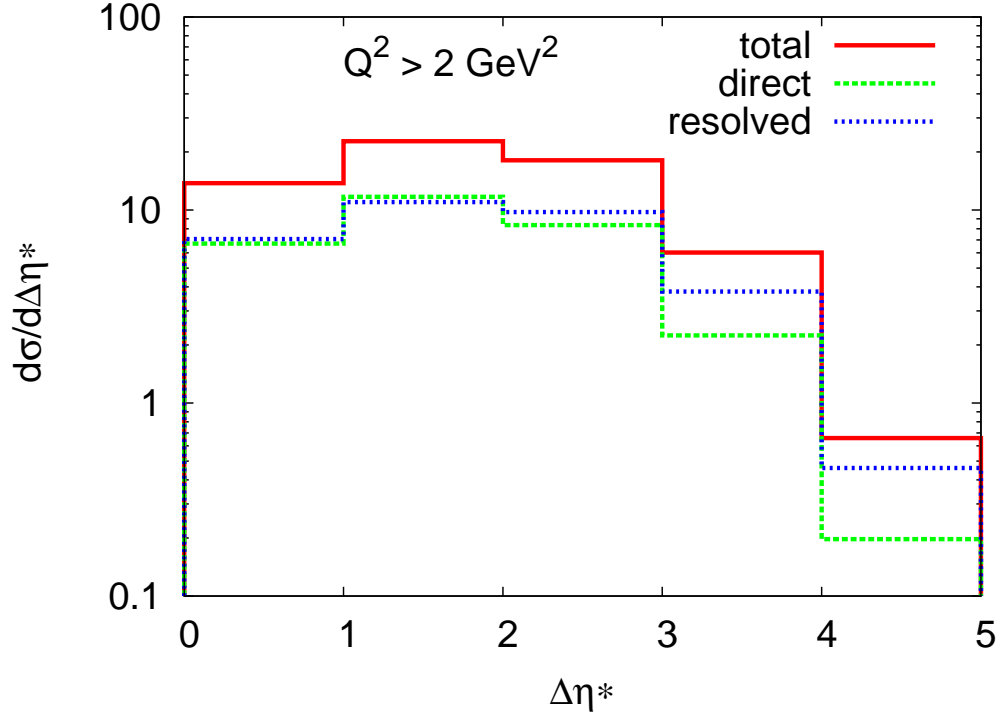


Figure 4: Variation of the cross section as a function of the rapidity gap between the forward pion and the largest p_{\perp} jet.

because of the extra convolution as explained above, y_2 is shifted to the right, and hence the whole resolved cross section, after averaging over Q^2 , y , y_1 and z is also shifted to the right.

There is a marked difference between the rapidity dependence of these cross sections and that of the dijet measured in ref. [28]. There, the dijet cross section is shown as a function of the rapidity gap between the two largest p_\perp jets measured in the CM* frame but no special requirement is imposed on the rapidity of one of the jets. The cross section is maximum at $\Delta\eta^* = 0$ and slowly decreases with increasing rapidity gap. The difference in shape with our results is due to the requirement that the π be observed in the forward direction, in the laboratory frame, which introduces strong kinematical constraints which distort, in our case, the rapidity dependence of the cross section. This is confirmed by later studies of the H1 Collaboration [31] where the rapidity dependence of the cross section between a forward jet and a di-jet system of small rapidity separation, is shown. A peak is observed at $\Delta\eta^* \sim 1$ with the cross section rapidly falling on either side. Let us note that this observable does not allow us to cover a large rapidity gap domain (about 2 units for the jet-dijet correlation instead of 5 in the particle-jet case).

We now present in Figs. 5 the cross section $d\sigma/d\Delta\eta^*$ where $\Delta\eta^*$ is the rapidity gap, still measured in the CM* frame, between the forward pion and the jet (with a minimum transverse momentum as specified above) which has the largest rapidity gap with the pion. The same general features as in Figs. 4 are observed with however a somewhat flatter behavior than before at medium rapidity gaps and a slower decrease at large gaps. This is related to the fact that the most backward jet is not necessarily the largest p_\perp one. This observable can be compared to the one discussed by the DØ collaboration where two jets with the largest separation are considered.

Let us now discuss some features of the NLO calculation. The HO corrections to the Born cross sections can be important in some kinematical domains. Consider, as an example, the “largest-rapidity-gap” case and the value $Q_{min}^2 = 10 \text{ GeV}^2$. For the direct contribution the ratio HO/Born is equal to 1/3 in the range $\Delta\eta^* \approx 0-1$ while, in the range $\Delta\eta^* = 4-5$, it reaches 20. This large variation is due to the opening of a new channel, namely $\gamma^*g \rightarrow q\bar{q}g$ (cf. Fig. 3(a)), which becomes important at large values of $\Delta\eta^*$. The variation of the ratio HO/Born is weaker in the resolved case: it varies from 1/3 to 4 for $\Delta\eta^*$ increasing from the range 0-1 to the range 4-5. This increase

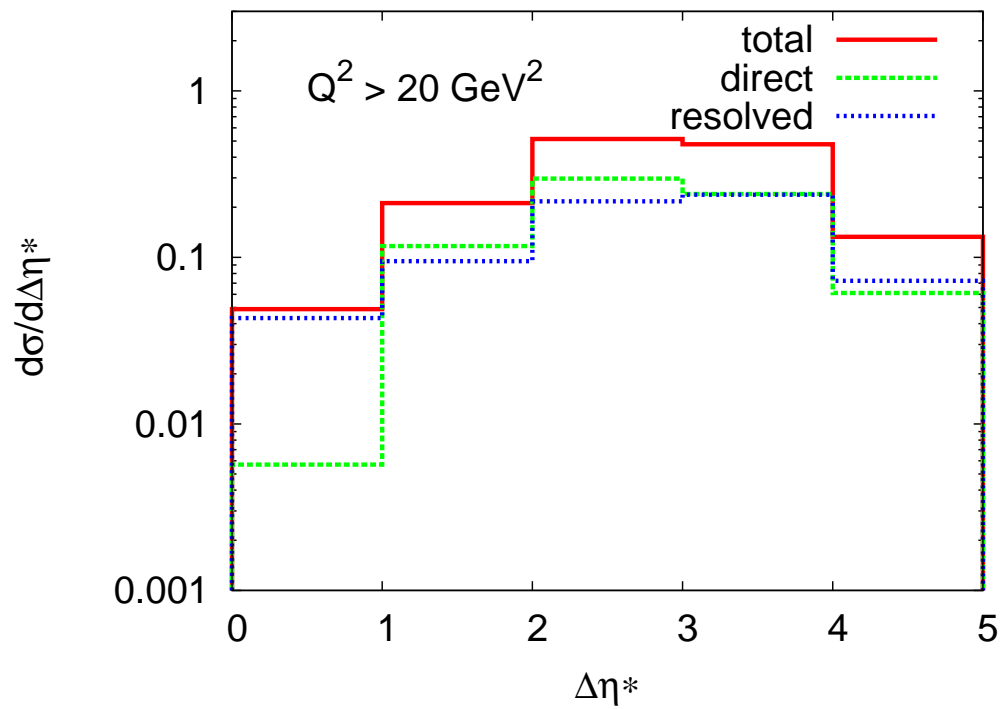
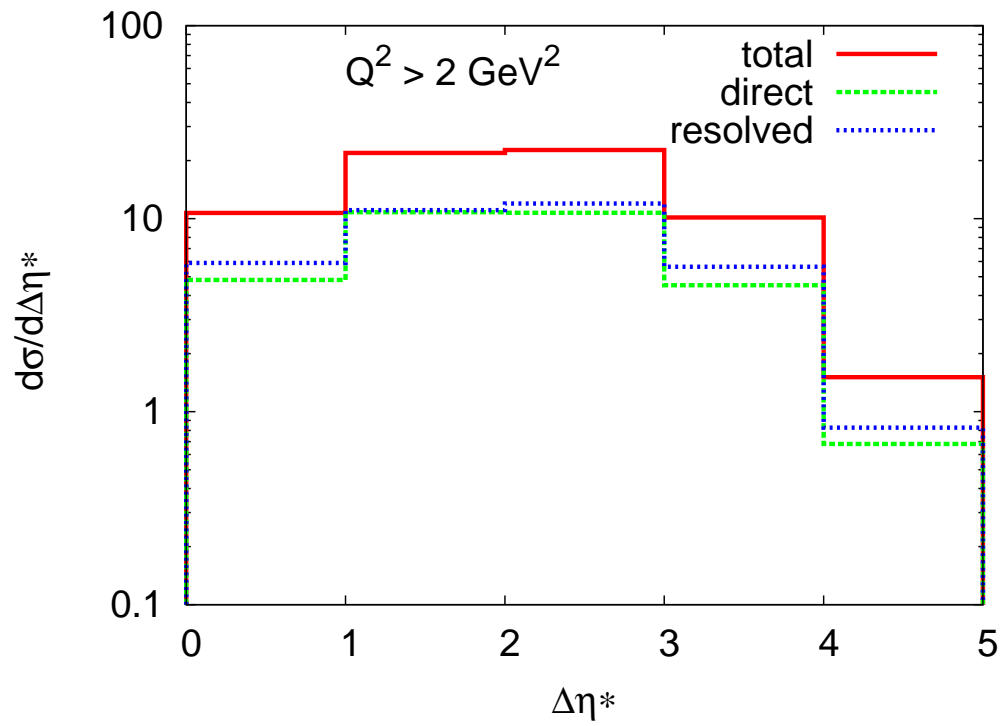


Figure 5: Variation of the cross section as a function of the rapidity gap between the forward pion and the jet with the largest rapidity gap with the pion.

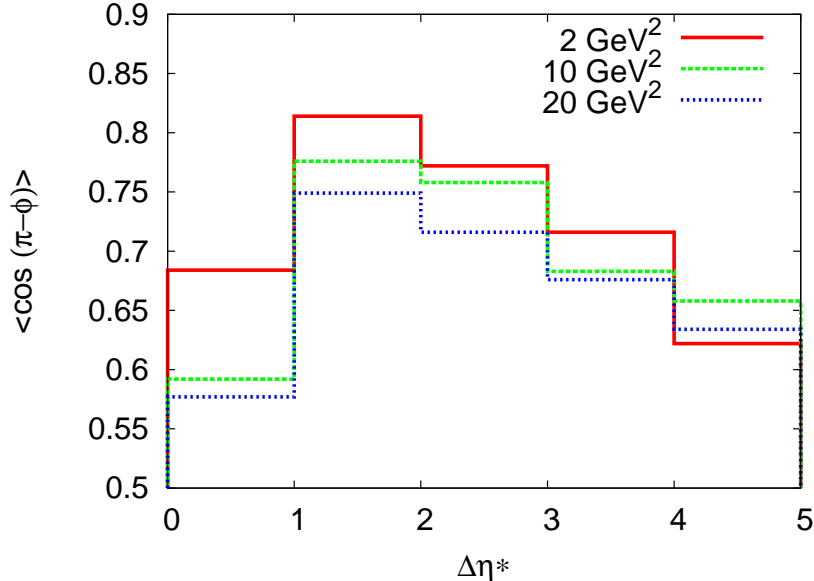


Figure 6: Average $\langle \cos(\pi - \phi) \rangle$ as a function of the rapidity gap between the forward pion and the most backward jet. The different curves correspond to the minimum values of Q^2 used in the calculation.

is due to the larger phase space available for the third jet when $\Delta\eta^*$ increases. This behavior of the ratio HO/Born partly explains those of the average $\langle \cos(\pi - \phi) \rangle$ which we now consider.

Figs. 6, 7[§] give the dependence of the average $\langle \cos(\pi - \phi) \rangle$ as a function of the rapidity gap under the same conditions as those of Fig. 5. The decrease of $\langle \cos(\pi - \phi) \rangle$ when $\Delta\eta^*$ increases is explained by the increase of the phase space available for the final jets in the $2 \rightarrow 3$ subprocesses. Going into the details of the underlying mechanisms we see in Fig. 7 that the direct component shows a more rapid decorrelation as $\Delta\eta^*$ increases because of the rapid growth of the HO contribution to this process. Comparing with the $D\bar{O}$ data of Fig. 1, we note that the overall size of $\langle \cos(\pi - \phi) \rangle$ is smaller for the same value of $\Delta\eta^*$ but that the slope is rather similar at large $\Delta\eta^*$.

Coming back to Fig. 6 it is interesting to note the decrease of $\langle \cos(\pi - \phi) \rangle$ when Q_{min}^2 increases. This corresponds to the $2 \rightarrow 3$ subprocesses becoming more isotropic. Finally the dip

[§]Note that the errors in Fig. 7 are large primarily because of the errors in the resolved case. As usual the errors in the cross section and the $\cos\phi$ weighted cross section have been added in quadratures to obtain the errors in the $\langle \cos(\pi - \phi) \rangle$ calculation.

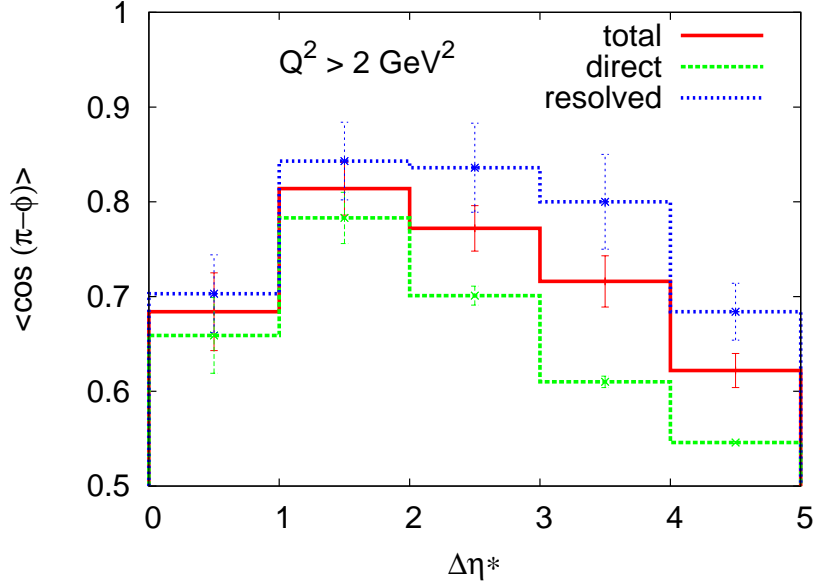


Figure 7: Detail of the components of $\langle \cos(\pi - \phi) \rangle$ as a function of the rapidity gap between the forward pion and the most backward jet for $Q^2 > 2 \text{ GeV}^2$.

at $\Delta\eta^*$ close to zero can be explained in the following way. First we note that in this $\Delta\eta^*$ range, the HO corrections are smaller than the Born term. In the direct case, they even become negative when Q_{min}^2 increases. In fact, this means that there are large compensations between the negative quasi $2 \rightarrow 2$ HO contributions (virtual and collinear) and the positive contributions coming from the $2 \rightarrow 3$ processes. When the $2 \rightarrow 3$ contributions are weighted by $\cos(\pi - \phi)$, the (weighted) HO contributions strongly decreases, which causes a decrease of $\langle \cos(\pi - \phi) \rangle$. For higher values of $\Delta\eta^*$, this effect is less pronounced. Let us also note that the resolved component is dominant in this bin for $Q^2 > 10 \text{ GeV}^2$. Without HO corrections to this component, we would have obtained $\langle \cos(\pi - \phi) \rangle \sim 1.0$

The behavior of $\langle \cos(\pi - \phi) \rangle$ with $\Delta\eta^*$ is strongly dependent on kinematical constraints, which are exactly respected in our NLO calculation, and this effect is specially strong near $\Delta\eta^* \sim 0$. On the other hand the BFKL approach does not usually implement total energy momentum conservation[¶] and we expect quite different predictions.

[¶]For a discussion see ref. [8].

4 Conclusion

In this work we compare the azimuthal decorrelation effects, as a function of the rapidity gap between two jets at the Tevatron and between a forward π^0 and a jet at HERA, using a next to leading order formalism. In the case of hadronic collisions, the calculated decorrelation effect is slightly slower than the data but it is still compatible with them taking into account statistical and systematic errors. In the deep inelastic case, the decorrelation is somewhat stronger than in the $p\bar{p}$ case, increasing with Q^2 , and we note interesting kinematical effects, related to the requirement of a forward particle trigger. In particular, it introduces a dip in the cross section at small rapidity gap, between the hadron and the jet. Dynamical effects and kinematical constraints also lead to very specific variations of $\langle \cos(\pi - \phi) \rangle$ with $\Delta\eta^*$.

References

- [1] L. N. Lipatov, Sov. J. Nucl. Phys. **23**, 338 (1976) [Yad. Fiz. **23**, 642 (1976)]. E. A. Kuraev, L. N. Lipatov and V. S. Fadin, Sov. Phys. JETP **44**, 443 (1976) [Zh. Eksp. Teor. Fiz. **71**, 840 (1976)]. I. I. Balitsky and L. N. Lipatov, Sov. J. Nucl. Phys. **28**, 822 (1978) [Yad. Fiz. **28**, 1597 (1978)].
- [2] A. H. Mueller and H. Navelet, Nucl. Phys. B **282**, 727 (1987).
- [3] V. Del Duca and C. R. Schmidt, Phys. Rev. D **49**, 4510 (1994) [arXiv:hep-ph/9311290].
- [4] W. J. Stirling, Nucl. Phys. B **423**, 56 (1994) [arXiv:hep-ph/9401266].
- [5] Yu. L. Dokshitzer, JETP **73**, 1216 (1971); V. N. Gribov and L. N. Lipatov, Sov. J. Nucl. Phys. **15**, 438 (1972) [Yad. Fiz. **15**, 781 (1972)]; G. Altarelli and G. Parisi, Nucl. Phys. B **126**, 298 (1977).
- [6] V. Del Duca and C. R. Schmidt, Phys. Rev. **D51**, 2150 (1995); V. Del Duca and C. R. Schmidt, in *QCD 94*, Proceedings of the International Conference, Montpellier, France, 1994, edited by S. Narison [Nucl. Phys. B (Proc. Suppl.) **B39**, C137 (1995)], presented at the *6th Rencontres de Blois*, Blois, France, 1994 (unpublished).

- [7] C. R. Schmidt, Phys. Rev. Lett. **78**, 4531 (1997) [arXiv:hep-ph/9612454].
- [8] L. H. Orr and W. J. Stirling, Phys. Rev. D **56**, 5875 (1997) [arXiv:hep-ph/9706529].
- [9] A. Sabio Vera and F. Schwennsen, Nucl. Phys. B **776**, 170 (2007) [arXiv:hep-ph/0702158].
- [10] S. Abachi *et al.* [D0 Collaboration], Phys. Rev. Lett. **77**, 595 (1996) [arXiv:hep-ex/9603010];
DØ Collaboration, A. Gossiou, presented at the *International Europhysics Conference on High Energy Physics*, Jerusalem, 1997
- [11] W. T. Giele, E. W. N. Glover and D. A. Kosower, Phys. Rev. Lett. **73**, 2019 (1994) [arXiv:hep-ph/9403347].
- [12] G. Marchesini and B. R. Webber, Nucl. Phys. B **310**, 461 (1988); I. G. Knowles, Nucl. Phys. B **310**, 571 (1988); G. Marchesini, B. R. Webber, G. Abbiendi, I. G. Knowles, M. H. Seymour and L. Stanco, Comput. Phys. Commun. **67**, 465 (1992).
- [13] A. H. Mueller, Nucl. Phys. Proc. Suppl. **18C**, 125 (1991).
- [14] C. Adloff *et al.* [H1 Collaboration], Nucl. Phys. B **538**, 3 (1999) [arXiv:hep-ex/9809028].
- [15] A. Aktas *et al.* [H1 Collaboration], Eur. Phys. J. C **36**, 441 (2004) [arXiv:hep-ex/0404009].
- [16] ZEUS Collaboration, J. Breitweg *et al.*, Eur. Phys. J. C **6**, 239 (1999), [hep-ex/9805016].
- [17] J. Kwiecinski, A. D. Martin and J. J. Outhwaite, Eur. Phys. J. C **9**, 611 (1999) [arXiv:hep-ph/9903439].
- [18] P. Aurenche, R. Basu, M. Fontannaz and R. M. Godbole, Eur. Phys. J. C **34**, 277 (2004) [arXiv:hep-ph/0312359].
- [19] M. Fontannaz, Eur. Phys. J. C **38**, 297 (2004) [arXiv:hep-ph/0410021].
- [20] P. Aurenche, R. Basu, M. Fontannaz and R. M. Godbole, Eur. Phys. J. C **42**, 43 (2005) [arXiv:hep-ph/0504008].
- [21] A. Daleo, C. A. Garcia Canal and R. Sassot, Nucl. Phys. **B662**, 334 (2003), [hep-ph/0303199].

- [22] A. Daleo, D. de Florian and R. Sassot, Phys. Rev. **D71**, 034013 (2005), [hep-ph/0411212];
A. Daleo, C. A. Garcia Canal and R. Sassot, Eur. Phys. J. C **33**, S404 (2004).
- [23] B. A. Kniehl, G. Kramer and M. Maniatis, Nucl. Phys. B **711**, 345 (2005) [Erratum-ibid. B **720**, 231 (2005)] [arXiv:hep-ph/0411300].
- [24] Technical details on the NLO codes can be found on the site http://lappweb.in2p3.fr/lapth/PHOX_FAMILY/main.html; DIJET and DISPHOX are available upon request from M. Fontannaz at Michel.Fontannaz@th.u-psud.fr.
- [25] B. Abbott *et al.* [D0 Collaboration], Phys. Rev. Lett. **82**, 2451 (1999) [arXiv:hep-ex/9807018].
- [26] J. Pumplin, D. R. Stump, J. Huston, H. L. Lai, P. Nadolsky and W. K. Tung, JHEP **0207**, 012 (2002) [arXiv:hep-ph/0201195].
- [27] B. A. Kniehl, G. Kramer and B. Pötter, Nucl. Phys. **B582**, 514 (2000) [arXiv:hep-ph/0010289].
- [28] A. Aktas *et al.* [H1 Collaboration], Eur. Phys. J. C **37**, 141 (2004) [arXiv:hep-ex/0401010].
- [29] J. Bartels, V. Del Duca and M. Wusthoff, Z. Phys. C **76**, 75 (1997) [arXiv:hep-ph/9610450].
- [30] A. Sabio Vera and F. Schwennsen, Phys. Rev. D **77**, 014001 (2008) [arXiv:0708.0549 [hep-ph]];
A. Sabio Vera and F. Schwennsen, arXiv:hep-ph/0611151.
- [31] A. Aktas *et al.* [H1 Collaboration], Eur. Phys. J. C **46**, 27 (2006) [arXiv:hep-ex/0508055].